J|A|C|S
ARTICLES
Published on Web 01/06/2004

Role of the Spacer in the Singlet−Singlet Energy Transfer Mechanism (Förster vs Dexter) in Cofacial Bisporphyrins

Sébastien Faure,[†,‡] Christine Stern,[†] Roger Guilard,*[,†] and Pierre D. Harvey*[,‡]

Contribution from the LIMSAG UMR 5633, Université de Bourgogne, 6 bd Gabriel, 21100 Dijon, France, and Département de Chimie de l'Université de Sherbrooke, Sherbrooke J1K2R1 Québec, Canada

Received August 18, 2003; E-mail: roger.guilard@u-bourgogne.fr; p.harvey@usherbrooke.ca

Abstract: The cofacial bisporphyrins H_4DPS (DPS = 4,6-bis[5-(2,8,13,17-tetraethyl-3,7,12,18-tetramethylporphyrinyl)]dibenzothiophene), H_4DPO (DPO = 4,6-bis[5-(2,8,13,17-tetraethyl-3,7,12,18-tetramethylporphyrinyl)]dibenzofuran), H_4DPX (DPX = 4,5-bis[5-(2,8,13,17-tetraethyl-3,7,12,18-tetramethylporphyrinyl)]-9,9-dimethylxanthene), H_4DPA (DPA = 1,8-bis[5-(2,8,13,17-tetraethyl-3,7,12,18-tetramethylporphyrinyl)]-anthracene), and H_4DPB (DPB = 1,8-bis[5-(2,8,13,17-tetraethyl-3,7,12,18-tetramethylporphyrinyl)]biphenylene) have been monometalated by $Zn(OAc)_2 \cdot 2H_2O$ and by $GaCl_3$ to explore the singlet−singlet energy transfer from the photoexcited metal porphyrin center to the linked free base porphyrin. The spectroscopic (UV−vis and fluorescence) and photophysical properties (fluorescence lifetimes, τ_F, and quantum yields, Φ_F) have been investigated at 298 and 77 K in degassed 2-MeTHF for the donor−acceptor systems, (Zn)H_2DPS, (Zn)H_2DPO, (Zn)H_2DPA, (Zn)H_2DPX, and (Zn)H_2DPB, as well as for the bis-zinc complexes, $(Zn)_2$DPS, $(Zn)_2$DPO, $(Zn)_2$DPX, and $(Zn)_2$DPB, respectively, and the monoporphyrin derivatives, H_2P, (Zn)P, and (Ga−OMe)P (P^{2-} = 5-phenyl-2,8,13,17-tetraethyl-3,7,12,18-tetramethylporphyrin-dianion). The singlet−singlet energy transfer rate constants (K_{ET}) were obtained using $K_{ET} = (1/\tau_F - 1/\tau_F°)$, where $\tau_F°$ is the fluorescence lifetime of the corresponding bis-zinc(II) systems (or (Zn)P and (Ga−OMe)P) where no energy transfer occurs. The τ_F value for three bis-zinc(II) compounds varies from 1.69 to 2.01 ns and is 1.84 (at 298 K) and 3.20 ns (at 77 K) for (Ga−OMe)P. In the donor−acceptor bismacrocycles, depending on the spacer and the temperature, the fluorescence lifetimes decrease down to 50−240 ps. The K_{ET} values range from ∼4 to ∼21 (ns^{-1}) and have been analyzed considering both the Förster and the Dexter mechanisms. Using the $C_{meso}-C_{meso}$ distance parameters in the calculations, the Förster and Dexter mechanisms operate for DPS and DPO, and for DPA, DPX, and DPB spacer systems, respectively. The limit distance where one mechanism dominates over the other is estimated to be around 5−6 Å.

Introduction

A clear understanding of energy transfer processes between porphyrin macrocycles in biological systems is essential for designing efficient light-harvesting systems,[1] notably when the process (antenna effect) operates in the primary stage of the photochemical events.[2−6] Many reviews on the topics in this area already exist.[7−9] The energy transfer may occur via short (Dexter)[10] and long distance interactions (Förster).[11,12] Based on the literature,[7] the field of singlet−singlet energy transfer for bisporphyrin systems indicates that the dominant mechanism is Förster. This particularity is explained by the fact that most investigated systems so far include a donor held to an acceptor using a spacer that keeps these chromophores at long distances, favoring this mechanism. One of the greatest challenges in this area is to estimate where one mechanism switches to the other as the dominating process when the distance is varied in a systematic manner, without variation of other structural parameters as possible. Although literature on porphyrin donor−spacer−porphyrin acceptor systems is relatively rich in this area, the use of a spacer favoring the cofacial geometry is rather rare.[7] Such a structure should strongly promote short distance interactions (favoring the Dexter process), but the dipole−dipole interactions (Förster) are still effective.[13,14] The

† Université de Bourgogne.
‡ Université de Sherbrooke.

(1) Jordan, P.; Fromme, P.; Witt, H. T.; Klukas, O.; Seanger, W.; Krauss, N. *Nature (London, U. K.)* **2001**, *411*, 909−917.
(2) Prathapan, S.; Johnson, T. E.; Lindsey, J. S. *J. Am. Chem. Soc.* **1993**, *115*, 7519−7520.
(3) Kodis, G.; Liddell, P. A.; de la Garza, L.; Clausen, P. C.; Lindsey, J. S.; Moore, A. L.; Moore, T. A.; Gust, D. *J. Phys. Chem. A* **2002**, *106*, 2036−2048.
(4) Luo, C.; Guldi, D. M.; Imahori, H.; Tamaki, K.; Sakata, K. *J. Am. Chem. Soc.* **2000**, *122*, 6535−6551.
(5) Gust, D.; Moore, T. A.; Moore, A. L. *Acc. Chem. Res.* **1993**, *26*, 198−205.
(6) Gust, D.; Moore, T. A.; Moore, A. L. *Acc. Chem. Res.* **2001**, *34*, 40−48.
(7) Harvey, P. D. In *The Porphyrin Handbook II*; Kadish, K. M., Smith, K. M., Guilard, R., Eds.; Academic Press: San Diego, 2003; Vol. 18, pp 63−250.
(8) Aratani, N.; Osuka, A.; Cho, H. S.; Kim, D. *J. Photochem. Photobiol., C* **2002**, *3*, 25−52.
(9) Wasielewski, M. R. *Chem. Rev.* **1992**, *92*, 435−461.
(10) Dexter, D. L. *J. Chem. Phys.* **1953**, *21*, 836−850.
(11) Förster, T. *Naturwissenschaften* **1946**, *33*, 166−175.
(12) Förster, T. *T. Ann. Phys.* **1948**, *2*, 55−73.
(13) Turro, N. J. *Modern Molecular Photochemistry*; University Science Books: Sausalito, CA, 1991.

Table 1. Comparison of the UV−Vis Absorption Data of the Mono- and Bisporphyrin Compounds[a]

compound	λ_{max} (nm) ($\epsilon \times 10^{-3}$ M^{-1} cm^{-1})				
	Soret region	Q-bands			
H_2P	402 (154)	502 (15)	532 (8)	578 (6)	626 (4)
(Zn)P	410 (270)	540 (18)		576 (11)	
(Ga−OMe)P	408 (157)	538 (6)		576 (5)	
H_4DPS	398 (309.9)	502 (29.6)	536 (15.0)	570 (14.2)	622 (6.8)
$(Zn)H_2DPS$	402 (340.6)	502 (15.6)	534 (21.7)	570 (20.9)	624 (3.1)
$(Zn)_2DPS$	402 (473.6)	536 (32)		572 (29)	
$(Ga-OMe)H_2DPS$	402 (361.7)	502 (11.7)	536 (20.3)	574 (17.7)	622 (1.8)
H_4DPO	396 (260)	502 (24)	536 (12.0)	572 (1.1)	624 (5.0)
$(Zn)H_2DPO$	400 (383.5)	502 (15.7)	534 (22.2)	570 (21.6)	622 (2.7)
$(Zn)_2DPO$[17]	400 (512)	534 (30.6)		571 (29.6)	
$(Ga-OMe)H_2DPO$	402 (252.7)	502 (11.0)	536 (14.8)	574 (13.9)	622 (2.8)
H_4DPA	395 (190.5)	506 (14.1)	539 (5.1)	578 (6.0)	631 (3.3)
$(Zn)H_2DPA$[41]	399 (196.6)	507 (7.0)	539 (10.5)	575 (11.6)	630 (1.3)
H_4DPX	380 (200)	508 (12.0)	543 (5.4)	578 (6.0)	628 (3.3)
$(Zn)H_2DPX$	386 (268)	512 (9.5)	542 (11.7)	576 (12.0)	628 (2.0)
$(Zn)_2DPX$[17]	389 (290)	541 (14.3)		576 (13.2)	
$(Ga-OMe)H_2DPX$	388 (269.4)	510 (8.4)	542 (11.4)	580 (10.4)	628 (1.4)
H_4DPB	379 (173.9)	511 (6.3)	540 (2.0)	580 (3.4)	632 (1.8)
$(Zn)H_2DPB$[41]	388 (200.0)	518 (4.1)	542 (5.2)	581 (6.8)	633 (0.8)

[a] In CH_2Cl_2 at 298 K.

distance of 10 Å is normally accepted as the crossing point between the two mechanisms,[13] but this distance may change from spacer to spacer. Numerous groups, including Nocera's,[15−20] Guilard's,[21−24] Chang's,[25−27] and others,[28] have prepared different rigid spacers for the synthesis of cofacial bisporphyrin systems. By examining the crystallographically measured $C_{meso}-C_{meso}$ distances, one can realize that this series (H_4DPS (6.3 Å),[29] H_4DPO (5.53 Å),[17,30] H_4DPA (4.94 Å),[31] H_4DPX (4.32 Å),[17] and H_4DPB (3.80 Å)[30]) offers a unique opportunity to fine-probe the photophysical data for donor−acceptor bisporphyrin systems in a cofacial orientation. The possibility of estimating the distance where the dominant mechanism switches from Förster to Dexter, less for cofacial bisporphyrin donor−acceptors, is unprecedented.

We now wish to report the syntheses of novel bismacrocycle compounds to assemble together a series of cofacial donor−acceptor systems, mono-zinc(II) and mono-gallium(III) centers as energy donors, and the free bases as acceptor, along with their corresponding bismetalated derivatives and monoporphyrin model compounds. The singlet−singlet energy transfer rate constants (K_{ET}) are obtained and are analyzed according to the Förster and Dexter formulations. The limiting distance where one mechanism switches to the other is evaluated (∼5 to 6 Å). These K_{ET} data are also compared to literature and discussed.

Experimental Section

Materials. 1,8-Bis[(4,4′-diethyl-3,3′-dimethyl-2,2′-dipyrryl)methyl]-dibenzothiophene,[31] 3,3′-diethyl-5,5′-dimethyl-4,4′-dimethyl-2,2′-dipyrrylmethane,[32] H_4DPO,[15] H_4DPX,[16] H_4DPB,[27] H_4DPA,[26] and their metalated derivatives were synthesized using literature methods.[21,22,24] Unless otherwise stated, all reagents and solvents were used as received. 2-MeTHF was purchased from Aldrich (99+%, anhydrous and under inert gas). $GaCl_3$ was in 5% solution in CH_3COOH, and the solvent was removed under vacuum prior to use. PTSA (*p*-toluenesulfonic acid) and DDQ (2,3-dichloro-5,6-dicyano-*p*-benzoquinone) were purchased from Aldrich. Column chromatography was performed with neutral alumina (Merck; usually Brockmann Grade III, i.e., deactivated with 6% water) and silica gel (Merck; 70−120 mm) and monitored by thin-layer chromatography (Merck 60 F254 silica gel precoated sheets, 0.2 mm thick) and UV−vis spectrometry.

Apparatus. ^1H NMR spectra were recorded on a Bruker DRX-500 AVANCE spectrometer at the Centre de Spectrométrie Moléculaire de l'Université de Bourgogne. Microanalyses were performed at the Université de Bourgogne on a Fisons EA 1108 CHNS instrument. UV−vis spectra were recorded on a Varian Cary 50 spectrophotometer. Mass spectra were obtained in linear mode with a Bruker Proflex III MALDI-TOF mass spectrometer using dithranol as matrix. Emission and excitation spectra were obtained using a double monochromator Fluorolog 2 instrument from Spex. Fluorescence lifetimes were measured on a Timemaster model TM-3/2003 apparatus from PTI. The source was a nitrogen laser with high-resolution dye laser (fwhm ≈ 1500 ps), and the fluorescence lifetimes were obtained from deconvolution or distribution lifetimes analysis. Complementary measurements for $(Zn)H_2DPA$ were performed on a picosecond laser system (fwhm = 35 ps) at the University of Ottawa.[33,34] All samples were prepared under inert atmosphere (in a glovebox, P_{O2} < 1−3 ppm) by

(14) Valeur, B. *Molecular Fluorescence. Principles and Applications*; Wiley-VCH: Weinheim, 2002.
(15) Deng, Y.; Chang, C. J.; Nocera, D. G. *J. Am. Chem. Soc.* **2000**, *122*, 410−411.
(16) Chang, C. J.; Deng, Y.; Heyduk, A. F.; Chang, C. K.; Nocera, D. G. *Inorg. Chem.* **2000**, *39*, 959−966.
(17) Chang, C. J.; Baker, E. A.; Pistorio, B. J.; Deng, Y.; Loh, Z.-H.; Miller, S. E.; Carpenter, S. D.; Nocera, D. G. *Inorg. Chem.* **2002**, *41*, 3102−3109.
(18) Chang, C. J.; Deng, Y.; Peng, S.-M.; Lee, G.-H.; Yeh, C.-Y.; Nocera, D. G. *Inorg. Chem.* **2002**, *41*, 3008−3016.
(19) Chang, C. J.; Yeh, C.-Y.; Nocera, D. G. *J. Org. Chem.* **2002**, *67*, 1403−1406.
(20) Chng, L. L.; Chang, C. J.; Nocera, D. G. *J. Org. Chem.* **2003**, *68*, 4075−4078.
(21) Lopez, M. A. Ph.D. Thesis, Université de Bourgogne: Dijon, 1990.
(22) Tardieux, C. Ph.D. Thesis, Université de Bourgogne: Dijon, 1997.
(23) Collman, J. P.; Ha, Y.; Guilard, R.; Lopez, M. A. *Inorg. Chem.* **1993**, *32*, 1788−1794.
(24) Brandès, S. Ph.D. Thesis, Université de Bourgogne: Dijon, 1993.
(25) Chang, C. K.; Kuo, M.-S.; Wang, C.-B. *J. Heterocycl. Chem.* **1977**, *14*, 943−945.
(26) Chang, C. K.; Abdalmuhdi, I. *J. Org. Chem.* **1983**, *48*, 5388−5390.
(27) Chang, C. K.; Abdalmuhdi, I. *Angew. Chem., Int. Ed. Engl.* **1984**, *23*, 164−165.
(28) Collman, J. P.; Tyvoll, D. A.; Chng, L. L.; Fish, H. T. *J. Org. Chem.* **1995**, *60*, 1926−1931.
(29) From molecular modeling MOPAC (AM1).
(30) Bolze, F.; Gros, C. P.; Drouin, M.; Espinosa, E.; Harvey, P. D.; Guilard, R. *J. Organomet. Chem.* **2001**, *643−644*, 89−97.
(31) Bolze, F. Ph.D. Thesis, Université de Bourgogne: Dijon, 2001.
(32) Chong, R.; Clezy, P. S.; Liepa, A. J.; Nichol, A. W. *Aust. J. Chem.* **1969**, *22*, 229−238.
(33) Mohtat, N.; Cozens, F. L.; Scaiano, J. C. *J. Phys. Chem. B* **1998**, *102*, 7557−7562.
(34) Cosa, G.; Vinette, A. L.; McLean, J. R. N.; Scaiano, J. C. *Anal. Chem.* **2002**, *74*, 6163−6169.

dissolution of the different compounds in 2-MeTHF using 1 cm^3 quartz cells with septum (298 K) or standard 5 mm NMR tubes (77 K). Three different measurements (i.e., different solutions) have been performed for the photophysical data (quantum yields and lifetimes). The sample concentrations were chosen to correspond to an absorbance of 0.05. Each absorbance value was measured five times for better accuracy for the measurements of the quantum yields. The reference for quantum yield was H_2TPP ($\Phi = 0.11$),[35−37] and the quantum yield determination for H_2TPP ($\Phi = 0.11$) at 77 K was performed with (Pd)TPP ($\Phi = 0.17$; 77 K; MCH (methylcyclohexane)) as reference.[38,39]

H_4DPS. This compound was synthesized according to a modification of the literature.[30] Under inert atmosphere, 3,3′-diethyl-5,5′-dimethyl-4,4′-dimethyl-2,2′-dipyrrylmethane (4.62 g; 16 mmol) and 1,8-bis[(4,4′-diethyl-3,3′-dimethyl-2,2′-dipyrryl)methyl]dibenzothiophene (5 g; 7.8 mmol) were dissolved in MeOH (1 L, degassed 1 h under argon) and stirred for 30 min in the dark. A solution of PTSA (10 g; 52 mmol) in 200 mL of MeOH was added over a period of 24 h, and the solution was stirred for 24 h. DDQ (4 g) was then added, and stirring was continued for 1 h. The solvent was removed under vacuum, and the solid was dissolved in 200 mL of CH_2Cl_2. The organic layer was filtered through a pad of alumina (using CH_2Cl_2 as solvent). The second purple band was collected, and the solvent was evaporated. Crystallization in CH_2Cl_2/MeOH afforded a purple solid. Yield: 21% (1.9 g). ^{1}H NMR ($CDCl_3$): δ (ppm) 9.82 (s, 4H), 9.63 (s, 2H), 8.82 (m, 2H), 7.95 (m, 4H), 3.82 (m, 16H), 3.38 (s, 12H), 2.35 (s, 12H), 1.64 (t, 12H), 1.58 (t, 12H), −3.68 (s, 2H), −3.75 (s, 2H). Anal. Calcd: C, 80.24; H, 7.09; N, 9.85; S, 2.82. Found: C, 79.41; H, 7.05; N, 9.99; S, 2.83. MS (MALDI-TOF) *m*/*z* 1136 (M^+); calc $C_{76}H_{80}N_8S$ 1136 g mol^{-1}.

General Procedure for the Preparation of Mono-zinc Bisporphyrins. Under argon, 1.5 g of the free base bisporphyrin was dissolved in degassed CH_2Cl_2 (400 mL) and stirred under reflux. A solution of 350 mg of $Zn(OAc)_2{\cdot}2H_2O$ in MeOH (50 mL) was then added over a period of 6 h, and the reaction was monitored by UV−vis and TLC (disappearance of the free base bisporphyrin). After the solution was dried, the residue, dissolved in CH_2Cl_2, was purified by chromatography.

(Zn)H_2DPS and (Zn)$_2$DPS. Chromatographic purification: alumina, CH_2Cl_2/heptane 7:3. The first band was collected as (Zn)$_2$DPS, and the second one was collected as (Zn)H_2DPS. After the solvent was removed under vacuum, recrystallization in CH_2Cl_2/heptane afforded purple crystals for each compound.

(Zn)H_2DPS. Yield: 57% (900 mg). ^{1}H NMR ($CDCl_3$): δ (ppm) 9.80 (s, 2H), 9.79 (s, 2H), 9.59 (s, 2H), 8.82 (m, 2H), 7.97 (m, 4H), 3.79 (m, 16H), 3.36 (s, 12H), 2.34 (s, 12H), 1.61 (m, 12H), 1.57 (m, 12H), −3.73 (s, 1H), −3.82 (s, 1H). Anal. Calcd: C, 76.01; H, 6.55; N, 9.33; S, 2.67. Found: C, 76.01; H, 7.05; N, 9.20; S, 2.73. MS (MALDI-TOF) *m*/*z* 1199 (M^+); calc $C_{76}H_{78}N_8SZn$ 1198 g mol^{-1}. UV−vis data are summarized in Table 1.

(Zn)$_2$DPS. Yield: 7% (110 mg). ^{1}H NMR ($CDCl_3$): δ (ppm) 9.70 (s, 4H), 9.60 (s, 2H), 8.85 (m, 2H), 7.96 (m, 4H), 3.82 (m, 16H), 3.38 (s, 12H), 2.37 (s, 12H), 1.59 (t, 24H). Anal. Calcd: C, 72.20; H, 6.06; N, 8.86; S, 2.54. Found: C, 72.07; H, 6.26; N, 8.87; S, 2.55. MS (MALDI-TOF) *m*/*z* 1263 (M^+); calc $C_{76}H_{76}N_8SZn_2$ 1260 g mol^{-1}.

(Zn)H_2DPO. Chromatographic purification: alumina, CH_2Cl_2/heptane 7:3. The second band was collected, and the solvent was removed under vacuum. Recrystallization in CH_2Cl_2/heptane afforded (Zn)H_2DPO as purple crystals. Yield: 51% (810 mg). ^{1}H NMR ($CDCl_3$): δ (ppm) 9.68 (m, 4H), 9.49 (m, 2H), 8.65 (m, 2H), 7.77 (m, 4H), 3.77 (m, 16H), 3.31 (2s, 12H), 2.36 (2s, 12H), 1.53 (m, 24H), −3.95 (s, 1H), −4.02 (s, 1H). Anal. Calcd: C, 77.04; H, 6.64; N, 9.46. Found: C, 76.71; H, 6.89; N, 9.19. MS (MALDI-TOF) *m*/*z* 1183 (M^+); calc $C_{76}H_{78}N_8OZn$ 1183 g mol^{-1}.

Scheme 1

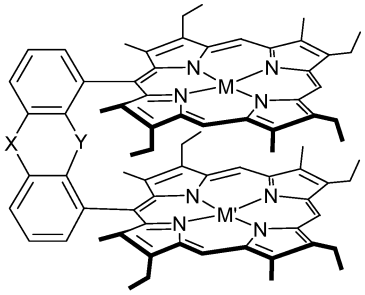

X = -, Y = S ; dibenzothiophene
M = 2H; M' = 2H; **H_4DPS**
M = Zn, Ga-OMe; M' = 2H; **(M)H_2DPS**
M = M' = Zn; **(Zn)$_2$DPS**

X = -, Y = O ; dibenzofuran
M = 2H; M' = 2H; **H_4DPO**
M = Zn, Ga-OMe; M' = 2H; **(M)H_2DPO**
M = M' = Zn; **(Zn)$_2$DPO**

X = C, Y = C ; anthracene
M = 2H; M' = 2H; **H_4DPA**
M = 2H; M' = Zn ; **(Zn)H_2DPA**

X = CMe_2, Y = O ; dimethylxanthene
M = 2H; M' = 2H; **H_4DPX**
M = Zn, Ga-OMe; M' = 2H; **(M)H_2DPX**
M = M' = Zn; **(Zn)$_2$DPX**

X = -, Y = - ; biphenylene
M = 2H; M' = 2H; **H_4DPB**
M = Zn; M' = 2H; **(Zn)H_2DPB**
M =M' = Zn; **(Zn)$_2$DPB**

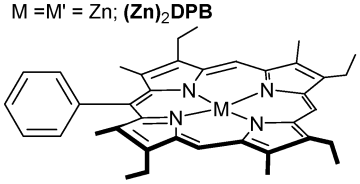

M = 2H; **H_2P**
M = Zn, Ga-OMe; **(M)P**

(Zn)H_2DPX. Chromatographic purification: alumina, CH_2Cl_2/heptane 8:2. The second band was collected, and the solvent was removed under vacuum. Recrystallization in CH_2Cl_2/heptane afforded (Zn)H_2DPX as purple crystals. Yield: 47% (740 mg). ^{1}H NMR ($CDCl_3$): δ (ppm) 9.10 (s, 1H), 9.00 (s, 1H), 8.50 (s, 2H), 8.40 (s, 2H), 7.86 (d, 2H), 7.23 (m, 2H), 6.99 (d, 2H), 4.14 (m, 4H), 4.14 (m, 4H), 3.55 (m, 4H), 3.33 (m, 4H), 2.26 (m, 12H), 2.21 (s, 6H), 1.70 (m, 12H), 1.40 (m, 12H), −7.07 (s, 1H), 7.23 (s, 1H). Anal. Calcd: C, 77.33; H, 6.90; N, 9.13. Found: C, 77.67; H, 6.48; N, 8.42. MS (MALDI-TOF) *m*/*z* 1225 (M^+); calc $C_{79}H_{84}N_8OZn$ 1225 g mol^{-1}.

General Procedure for the Preparation of Mono-gallium Bisporphyrin. After acetic acid was removed under vacuum, benzonitrile (40 mL), CH_3COONa (0.82 mg), and mono-zinc bisporphyrin (400 mg) were added to $GaCl_3$ (1.40 mL, 5% in acetic acid). The mixture was refluxed, and the reaction was monitored by UV−vis (disappearance of the mono-zinc bisporphyrin, ∼90 min). The solvent was removed under vacuum. CH_2Cl_2 (200 mL) and HCl 6 M (50 mL) were added, and the solution was stirred vigorously for 30 min. The organic layer was extracted, washed, and dried over $MgSO_4$. The solvent was removed to yield a dark solid, which was redissolved in CH_2Cl_2 and filtered through a pad of alumina (CH_2Cl_2/MeOH 95:5). The purple band was collected. Recrystallization in CH_2Cl_2/MeOH produced a pure mono-gallium derivative as a light purple solid.

(Ga−OMe)H_2DPS. Yield: 53% (220 mg). ^{1}H NMR ($CDCl_3$): δ (ppm) 9.88 (m, 2H), 9.76 (m, 2H), 9.60 (m, 2H), 8.84 (m, 2H), 8.02

(35) Strachan, J.-P.; Gentemann, S.; Seth, J.; Kalsbeck, W. A.; Lindsey, J. S.; Holten, D.; Bocian, D. F. *J. Am. Chem. Soc.* **1997**, *119*, 11191−11201.
(36) Gouterman, M. In *The Porphyrins*; Dolphin, D., Ed.; Academic Press: New York, 1978; Vol. III, pp 1−165.
(37) Seybold, P. G.; Gouterman, M. *J. Mol. Spectrosc.* **1969**, *31*, 1−13.
(38) Harriman, A. *J. Chem. Soc., Faraday Trans.* **1980**, *76*, 1978−1985.
(39) Murov, S. L.; Carmichael, I.; Hug, G. L. *Handbook of Photochemistry*, 2nd ed.; Marcel Dekker: New York, 1993.

Scheme 2

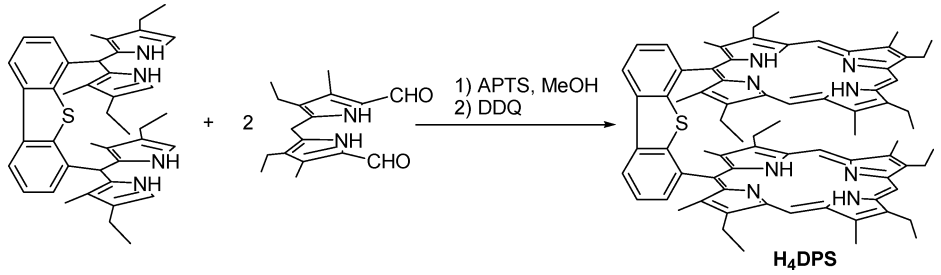

Scheme 3

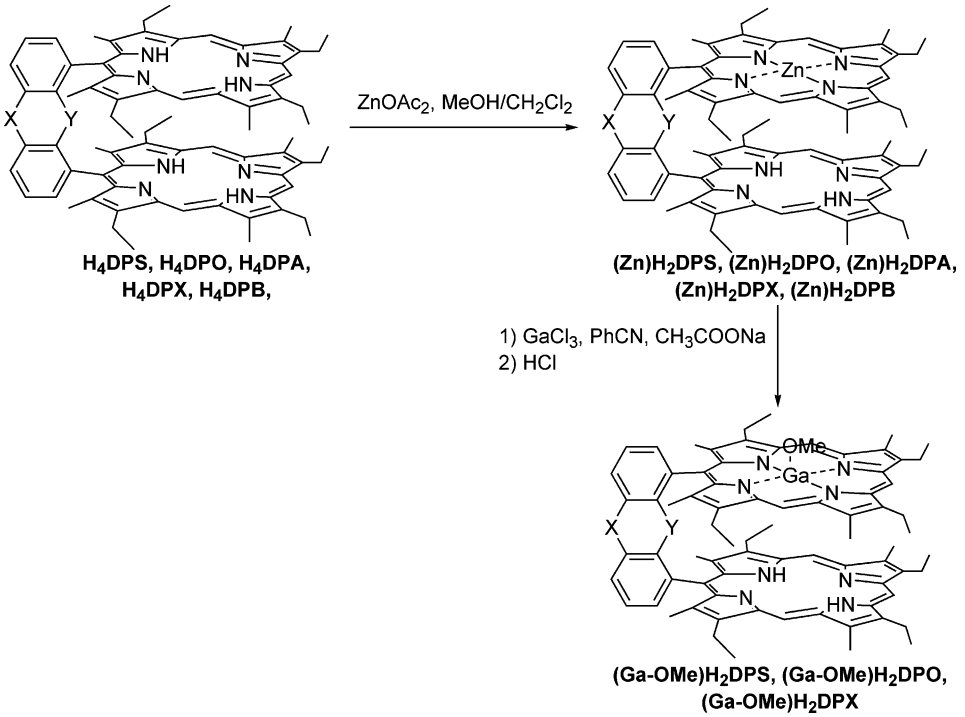

(m, 4H), 3.80 (m, 16H), 3.37 (s, 12H), 2.30 (m, 12H), 1.60 (m, 24H), −3.64 (2s, 3H), −3.78 (s, 1H), −3.85 (s, 1H). Anal. Calcd: C, 74.81; H, 6.60; N, 9.06; S, 2.59. Found: C, 74.33; H, 6.42; N, 8.92; S, 2.44. MS (MALDI-TOF) *m*/*z* 1205 (M^+ − OMe); calc $C_{76}H_{79}GaN_8S$ 1204 g mol^{-1}.

(Ga−OMe)H_2DPO. Yield: 47% (195 mg). ^{1}H NMR ($CDCl_3$): δ (ppm) 9.80 (m, 2H), 9.68 (m, 2H), 9.51 (m, 2H), 8.66 (m, 2H), 7.80 (m, 4H), 3.75 (m, 16H), 3.32 (m, 12H), 2.37 (m, 12H), 1.53 (m, 24H), −3.95 (s, 1H), −4.02 (s, 1H), −4.00 (2s, 3H). Anal. Calcd: C, 75.79; H, 6.69; N, 9.18. Found: C, 76.70; H, 6.89; N, 9.18. MS (MALDI-TOF) *m*/*z* 1188 (M^+ − OMe); calc $C_{76}H_{79}GaN_8O$ 1188 g mol^{-1}.

(Ga−OMe)H_2DPX. Yield: 33% (135 mg). ^{1}H NMR ($CDCl_3$): δ (ppm) 9.10 (s, 1H), 9.00 (s, 1H), 8.50 (s, 2H), 8.40 (s, 2H), 7.86 (d, 2H), 7.23 (m, 2H), 6.99 (d, 2H), 4.14 (m, 4H), 4.14 (m, 4H), 3.55 (m, 4H), 3.33 (m, 4H), 2.26 (m, 12H), 2.21 (s, 6H), 1.70 (m, 12H), 1.40 (m, 12H), −3.90 (s, 3H), −6,59 (s, 1H), 7.20 (s, 1H). Anal. Calcd: C, 76.12; H, 6.95; N, 8.88. Found: C, 75.97; H, 7.06; N, 8.42. MS (MALDI-TOF) *m*/*z* 1230 (M^+ − OMe); calc $C_{79}H_{85}GaN_8$ 1230 g mol^{-1}.

Results

Synthesis. The list of investigated compounds is shown in Scheme 1. The free bases were prepared according to established procedures,[40] except for H_4DPS. The latter was synthesized using a modified procedure as shown in Scheme 2. This more convenient and efficient synthetic procedure reduces the number of purification steps as previously reported.[30]

The general synthesis of the monometalated bisporphyrins is shown in Scheme 3 and proceeds first by incorporation of a zinc(II) cation into one of the porphyrin macrocycles, providing one series of donor−acceptor systems. A second metalation with gallium trichloride leads to heterobimetallic Zn−Ga bisporphyrins. Subsequently, the use of acid allows one to selectively remove all residual zinc(II) ion from the bismacrocycles, giving access to a second family of donor−acceptors. This two-step procedure is necessary as insertion of the gallium atom into the free base was unsuccessful in producing high yields of the monometalated product.[41]

The MALDI-TOF technique is well suited for the characterization of all investigated molecules. Considering the (Ga−OMe) porphyrin spectra, the data indicate the absence of the molecular ion peaks, but rather show fragments consistent with the targeted molecules that have lost the OMe fragment. This result illustrates the rather fragile Ga−OMe bond.

Absorption Spectra. Table 1 summarizes the UV−vis data for all investigated porphyrin compounds, for which the Soret-

(40) Kadish, K. M., Smith, K. M., Guilard, R., Eds. *The Porphyrin Handbook*; Academic Press: New York, 2000.

(41) Guilard, R.; Lopez, M. A.; Tabard, A.; Richard, P.; Lecomte, C.; Brandès, S.; Hutchison, J. E.; Collman, J. P. *J. Am. Chem. Soc.* **1992**, *114*, 9877−9889.

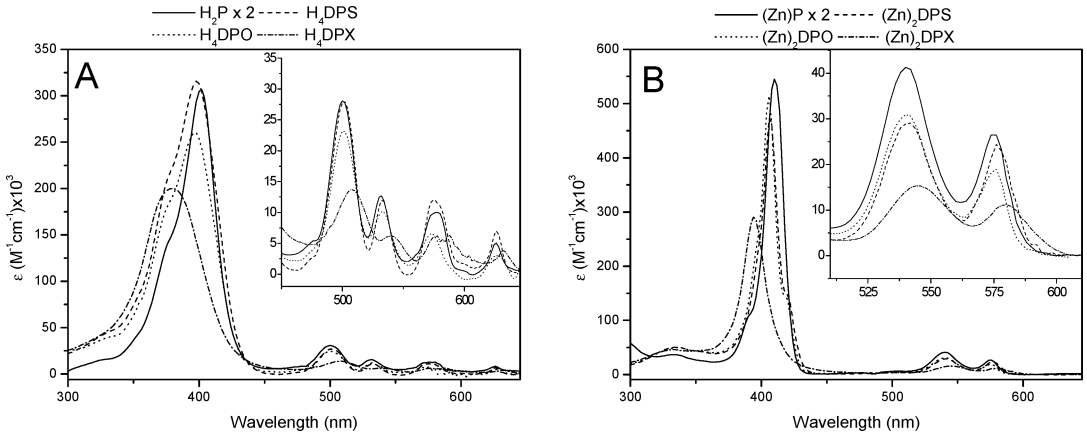

Figure 1. UV−vis spectra of (A) $H_2P \times 2$ as compared to the free base bisporphyrins H_4DPS, H_4DPO, and H_4DPX and (B) (Zn)P × 2 as compared to the corresponding bis-zinc(II) bisporphyrins (298 K, CH_2Cl_2).

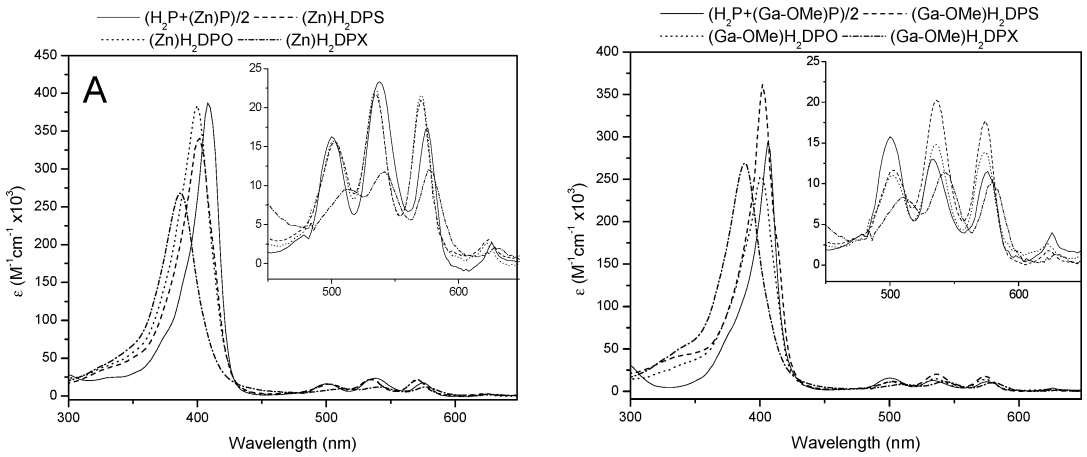

Figure 2. UV−vis spectra of (H_2P + (M)P)/2 as compared to the monometalated bisporphyrins (M)H_2DPS, (M)H_2DPO, and (M)H_2DPX where (A) M = Zn and (B) M = Ga−OMe (298 K, CH_2Cl_2).

and Q-bands are characterized. Figure 1 shows the comparison between the UV−vis spectra for H_4DPO, H_4DPS, and H_4DPX with H_2P, and $(Zn)_2$DPO, $(Zn)_2$DPS, and $(Zn)_2$DPX with (Zn)P, where clear discrepancies are shown. The most remarkable feature is the fact that the absorption spectra for the monoporphyrin and bisporphyrin species are not superimposable.[25,42] A dependence of the Soret band λ_{max} and bandwidth is observed and varies as P > DPS > DPO > DPA > DPX > DPB for λ_{max} (Table 1) and in reverse for the bandwidth. This trend is in agreement with variable intermacrocycle interactions due to the increase of the C_{meso}−C_{meso} distance (DPB < DPX < DPA < DPO < DPS), but there was no splitting of the band due to excitonic coupling. The same observation and conclusion are made for the donor−acceptor bisporphyrin series (both Zn/H_2 and Ga/H_2 as shown in Figure 2) where the comparison is made with the 1:1 spectral algebraic sum of (Zn)P and H_2P (and (Ga−OMe)P and H_2P) monoporphyrins. At 77 K, the spectra of (Zn)H_2DPS and (Zn)H_2DPO are better resolved. Moreover, the half sum of the bis-free base and bis-zinc(II) bisporphyrin spectra almost superimpose the spectra of the corresponding monometalated bisporphyrins (see Supporting Information). This feature indicates that the interporphyrin interactions for both spacers are rather weak. In comparison, the absorption spectra for (Zn)H_2DPA, (Zn)H_2DPX, and (Zn)H_2DPB are not resolved at low temperature due to the strong interaction between the two chromophores.

(42) Chang, C. K. *J. Heterocycl. Chem.* **1977**, *14*, 1285−1288.

Fluorescence. Table 2 summarizes the fluorescence spectroscopic (λ_{max}) and quantum yield data (Φ_F), along with some other relevant data, and Figure 3 shows typical examples of fluorescence spectra. The fact that the excitation spectra superimpose the absorption spectra confirms the identity of the fluorescence. The quantum yields for H_2P, H_4DPS, and H_4DPO, as well as for (Zn)P, $(Zn)_2$DPS, and $(Zn)_2$DPO, respectively, compare favorably, indicating the absence of strong intramolecular interactions in the excited state. Conversely, for all of the DPA, DPX, and DPB systems, the corresponding Φ_F values decrease as the chromophores get closer to each other (C_{meso}−C_{meso} distance: DPB < DPX < DPA). Those results are consistent with the presence of stronger interporphyrin interactions. At first glance, DPS and DPO behave similarly, and DPA, DPX, and DPB form a different series of bis-chromophores. The fluorescence spectra for the monometalated bisporphyrins show a drastic decrease in relative intensity for the zinc(II) porphyrin emission versus the free base fluorescence, as illustrated in Figures 3 and 4. The weak 0−0 fluorescence peak is barely perceptible in the spectra, even at 77 K, due to a singlet−singlet energy transfer from the zinc(II) porphyrin to the free base, which is now addressed in more detail.

Energy Transfer. The energy transfer rate (K_{ET}) from the photoexcited metal (Zn or Ga) porphyrin to the free base porphyrin subunit in each momometalated bisporphyrin was assessed using picosecond fluorescence spectroscopy. The photophysical data are analyzed according to the energy transfer

Table 2. Luminescence Data for the Mono- and Bisporphyrins[a]

compound		quantum yields[d]		λ_{max} (nm)[e]	
macrocycle	metal or H	298 K	77 K	298 K	77 K
P	2H	0.0892	0.0862	629, 696	623, 690
	Zn[b]	0.0214	0.0266	580, 635	581, 639, 721
	Ga[b]	0.0173	0.0541	581, 637	579, 637, 718
DPS	4H	0.0887	0.0838	629, 697	623, 689
	Zn, 2H[c]	0.1070	0.0909	583, 628, 697	585, 622, 689
	2Zn[b]	0.0203	0.0226	581, 636	583, 643, 720
	Ga, 2H[c]	0.0788	0.1038	582, 629, 697	582, 622, 689
DPO	4H	0.0937	0.0786	628, 697	623, 691
	Zn, 2H[c]	0.0989	0.0639	631, 697	581, 622, 690
	2Zn[b]	0.0294	0.0347	580, 635	584, 643, 722
	Ga, 2H[c]	0.0909	0.0643	628, 697	621, 698
DPA	4H	0.020[30]	0.044[30]	634[30]	624[30]
	Zn, 2H[c]	0.1070	0.0882	585, 630, 698	620, 688
DPX	4H	0.0361	0.0643	635, 701	637, 702
	Zn, 2H[c]	0.0190	0.0707	587, 641, 704	588, 639, 707
	2Zn[b]	0.0115	0.0234	584, 643	595, 649, 721
	Ga, 2H[c]	0.0666	0.0271	588, 639, 705	588, 638, 708
DPB	4H	0.0040[30]	0.012[30]	641[30]	636[30]
	Zn, 2H[c]	0.053	0.0392	623, 690	617, 693
	2Zn[b]	0.006	0.0108	643	607, 659, 733

[a] In 2-MeTHF, λ_{exc} = 500 nm, the reference for quantum yield was H_2TPP 0.11,[35−37] the quantum yield for H_2TPP (0.11) at 77 K was verified with (Pd)TPP (0.17; 77 K; MCH) as a reference.[38,39] [b] Excitation 540 nm. [c] Total quantum yield of the fluorescence and 85% of the absorbance are due to the free base porphyrin. [d] The uncertainties of the quantum yields are ±10%. [e] The uncertainties of the λ_{max} are ±1 nm.

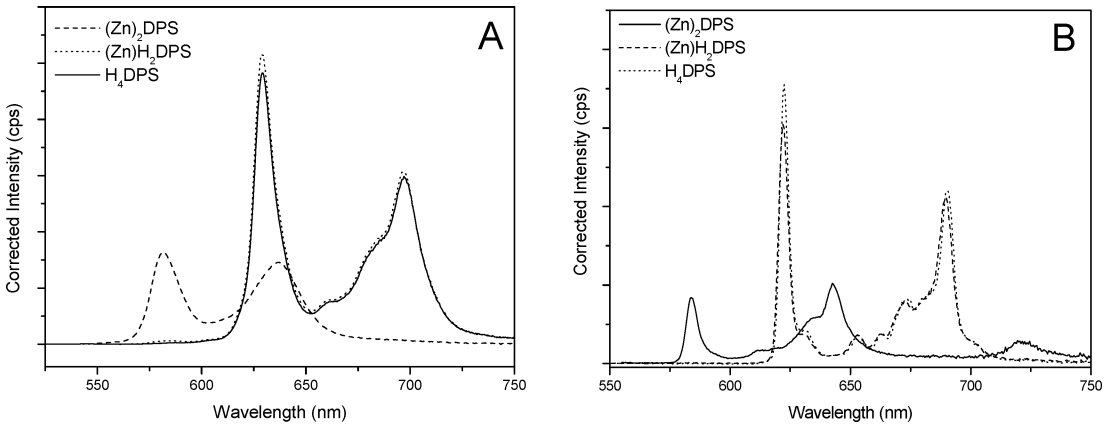

Figure 3. Fluorescence spectra of $(Zn)_2$DPS, $(Zn)H_2$DPS, and H_4DPS in 2-MeTHF (A, 298 K; B, 77 K).

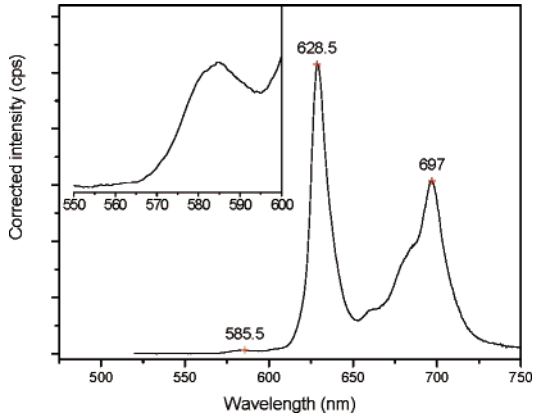

Figure 4. Emission spectrum of $(Zn)H_2$DPS in 2-MeTHF at 298 K (inset: the weak fluorescence at 585 nm arising from the zinc(II) porphyrin donor).

process as described in Scheme 4. Because of the difficulty in measuring Φ_F accurately for the donor chromophore, the fluorescence lifetimes (τ_F) are studied (Table 3). In fact, the absorbance related to the Zn(II)P fragment is difficult to evaluate at a given wavelength (the Zn(II)P fragment absorbs in the same region as the H_2P chromophore), and its emission is too weak (see inset in Figure 4). The K_{ET} values are calculated using eq 1:

$$K_{ET} = \left(\frac{1}{\tau_F} - \frac{1}{\tau_F^0}\right) \quad (1)$$

where τ_F^0 is the fluorescence lifetime of closely related bis-macrocycles where no energy transfer occurs. The zinc(II) models are the corresponding $(Zn)_2$DPS, $(Zn)_2$DPO, $(Zn)_2$DPX, $(Zn)_2$DPB, and, for $(Zn)_2$DPA, (Zn)P. For the gallium(III) series, (Ga−OMe)P is preferred: the bis-gallium series were excluded from this work as they all exhibit a double fluorescence (two λ_{max} and two τ_F).[31,43] Table 3 summarizes the τ_F, τ_F^0, and K_{ET} data. We were not able to reproduce the data, notably $(Zn)H_2$DPA and $(Zn)H_2$DPB, obtained by Osuka and collabora-

(43) Harvey, P. D.; Proulx, N.; Martin, G.; Drouin, M.; Nurco, D. J.; Smith, K. M.; Bolze, F.; Gros, C. P.; Guilard, R. *Inorg. Chem.* **2001**, *40*, 4134−4142.

Scheme 4

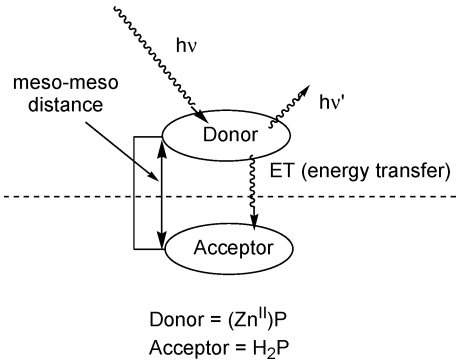

Table 3. Fluorescence Lifetime and Singlet–Singlet Energy Transfer Rate Constants for the Bisporphyrins[a]

compound		lifetime (ns)[b]		K_{ET} (ns^{-1})	
macrocycle	metal or H	298 K	77 K	298 K	77 K
P	2H	17.3	23.3		
	Zn	1.70	1.94		
	Ga	1.84	3.2		
DPS	4H	18.0	23.6[30]		
	Zn, 2H[c]	0.19	0.19	4.7	4.6
	2Zn	1.95	1.85		
	Ga, 2H[c]	0.24	0.20	3.7	4.8
DPO	4H	18.5	20.7[30]		
	Zn, 2H[c]	0.18	0.16	5.0	5.9
	2Zn	1.69	2.01		
	Ga, 2H[c]	0.09	0.16	11	6.0
DPA	4H	13.7	24[30]		
	Zn, 2H[c]	0.14	0.13	6.4	7.2
DPX	4H	14.1	17.0[30]		
	Zn, 2H[c]	0.10	0.09	9.8	10.9
	2Zn	1.73	1.94		
	Ga, 2H[c]	0.14	0.14	6.4	7.0
DPB	4H	11.7	17.0[30]		
	Zn, 2H[c]	0.05	0.06	20.8[42]	15.4
	2Zn	0.63	1.80		

[a] In 2-MeTHF. [b] The uncertainties in lifetime are ±10%. [c] Lifetime for metalated porphyrin.

tors.[44] Longer τ_F's were found despite the fact that the measurements were reproduced several times on two different instruments (described in the Experimental Section). In addition, the K_{ET} values were also estimated using the Φ_F data (eq 2):

$$K_{ET} = \left(\frac{1}{\Phi_F} - \frac{1}{\Phi_F^0}\right) \times \frac{\Phi_F^0}{\tau_F^0} \qquad (2)$$

where Φ_F is the fluorescence quantum yield, and τ_F^0, Φ_F^0 are the fluorescence lifetime and quantum yield of closely related bismacrocycles where no energy transfer occurs. These data agree within the uncertainties of the K_{ET} values calculated according to eq 1.[45] The key features are as follows: (1) the 77 K data are considered more accurate as the fluorescence signals become sharper inducing an easier discrimination of the (Zn)P contribution from the overall decay traces, (2) the τ_F data follow Φ_F trends (as τ_F decreases, Φ_F decreases as well), (3) there is a dependence of K_{ET} on the $C_{meso}-C_{meso}$ distance (as the distance decreases, K_{ET} increases), and (4) within the uncertainty, K_{ET} is not sensitive to the nature of the metal (Zn vs Ga).

Discussion

As dipole–dipole interaction (Förster) and exchange (Dexter) mechanisms are possible for singlet–singlet energy transfer, the K_{ET} data are analyzed according to the Förster[11,12] (eq 3)[14] and Dexter[10] (eq 4)[14] formulations

$$K_{ET}^{\text{Förster}} = k_D R_F^6 \left(\frac{1}{R}\right)^6 \qquad (3)$$

$$K_{ET}^{\text{Dexter}} = \frac{2\pi}{h} K J' \exp\left(\frac{-2R}{L}\right) \qquad (4)$$

where k_D is the emission rate constant for the donor, R_F is the Förster radius, that is, the distance at which transfer and spontaneous decay of excited donors are equally probable, R is the distance between the two macrocycles, J' is the integral overlap, K is an experimental constant, and L is the average Bohr radius ($L = 4.8$ for porphyrin[7,46]). Simulated graphs (using arbitrary values for k_D, R_F, J', and K) are shown in Figure 5. The straight lines represent what is expected for an energy transfer rate operating exactly (and uniquely) according to a Förster (graph A) and Dexter (graph B) mechanism. It is noteworthy to state that the line in the Förster equation must pass through the origin (0,0). The curved lines in each of these graphs are simulated lines obtained with eqs 3 (Förster) or 4 (Dexter), but transposed onto the other graph (i.e., Förster equation plotted against Dexter formulation and vice versa). From these graphs, the zones where the Förster and Dexter mechanisms are dominant (bold lines) are easily distinguishable. The experimental K_{ET} data are plotted against $1/R^6$ and $\exp(-2R/4.8)$ at 77 K in Figure 6. These graphs show striking similarities to those of Figure 5, providing clear evidence that both mechanisms operate for these five donor–acceptor bisporphyrins. At 298 K, a similar behavior is noted (Supporting Information), but the 77 K τ_F data are of better quality.

The energy transfer for (Zn)H_2DPS and (Zn)H_2DPO proceeds dominantly according to a Förster mechanism, while the transfer in (Zn)H_2DPB, (Zn)H_2DPX, and (Zn)H_2DPA occurs mainly via a Dexter mechanism. This observation is consistent with the relative presence of intramolecular porphyrin–porphyrin interactions as deduced from the spectroscopic and photophysic data. The change of dominant mechanism for energy transfer in this series occurs between (Zn)H_2DPO and (Zn)H_2DPA. By extrapolating a line down to $K_{ET} = 0$ for the Dexter plot (Figure 6, graph B), we located the critical R_0 distance where the Dexter process no longer operates, between 5 and 6 Å, taking into account the uncertainties. Again, the $C_{meso}-C_{meso}$ distance is 4.94 and 5.53 Å, for DPA and DPO, respectively, a range that overlaps with the graphically estimated R_0 value. In that respect, the closest study related to this investigation is the work reported by Osuka et al.[44] In this previous work, a large series of Zn-porphyrin/spacer/free porphyrin donor–acceptor systems where

(44) Osuka, A.; Maruyama, K.; Yamazaki, I.; Tamai, N. *Chem. Phys. Lett.* **1990**, *165*, 392–396.

(45) The main conclusion of this work is that the Förster and Dexter mechanisms switch at a given distance (~5–6 Å). These results have just been reproduced by ongoing investigations on T_1-T_1 energy transfers in (Pd)H_2- and (ZnPd)-bisporphyrins. In this case, only the Dexter mechanism operates at the triplet state where, at a given distance, an "on/off situation" should occur. This "critical" value is the same as that determined in this work, and this investigation will be reported in due course.

(46) Fillers, J. P.; Ravichandran, K. G.; Abdalmuhdi, I.; Tulinsky, A.; Chang, C. K. *J. Am. Chem. Soc.* **1986**, *108*, 417–424.

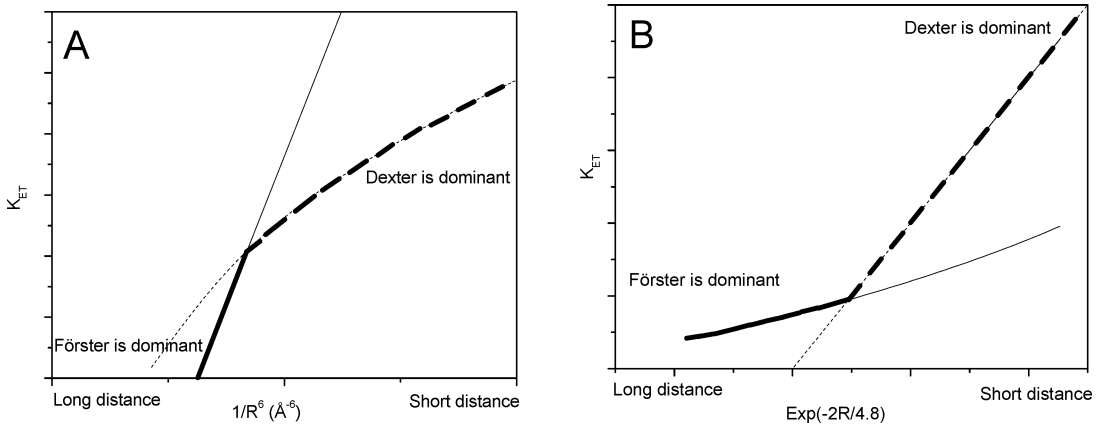

Figure 5. Qualitative theoretical plots for K_{ET} versus $1/R^6$ (Förster, graph A) and K_{ET} versus exp($-2R/4.8$) (Dexter, graph B). The solid lines correspond to hypothetical situations where the Förster mechanism operates, while the dotted lines are hypothetical situations for the Dexter mechanism.

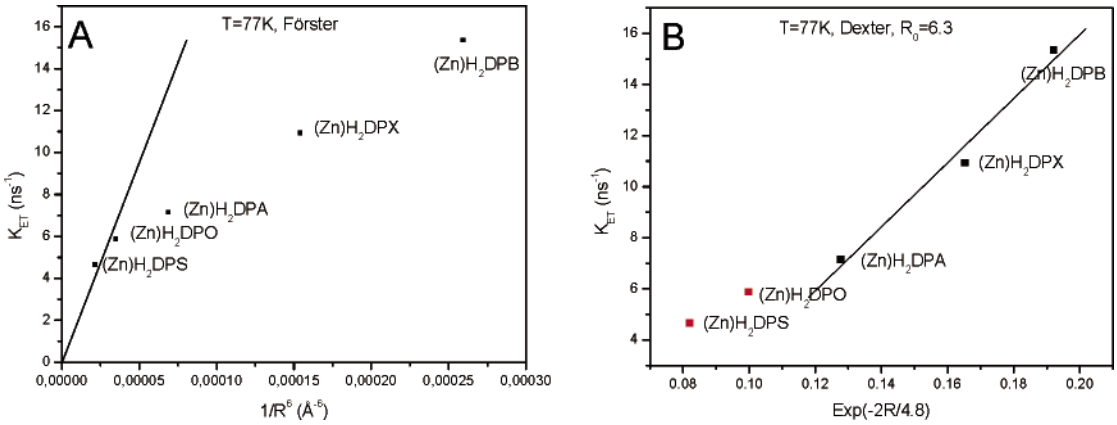

Figure 6. Plot of K_{ET} versus $1/R^6$ and K_{ET} versus exp($-2R/4.8$). The straight lines are associated with the molecules operating with the Förster (graph A) and Dexter (graph B) mechanism, respectively.

the spacers are various benzenyl (*para*- and *meta*-), naphthalenyl, anthracenyl, biphenyl, alkyl, and rigid polycyclic saturated fragments were investigated. A center-to-center distance dependence on the K_{ET} was reported and interpreted with a Förster mechanism, which is consistent with the rather long distances between the donor and acceptor induced by these spacers. The (Zn)H_2DPA bismacrocycle, which is common in both works, is a donor−acceptor system that exhibits a K_{ET} located at the limit between the Förster and Dexter regions according to our results. However, this system exhibits the fastest rate in Osuka's work, which places a data point at the limit of a plot ln(K_{ET}) versus center-to-center distance. Any small deviation from linearity could have been missed taking into account the uncertainties.

Table 4[47−50] compares singlet−singlet K_{ET} data for selected bisporphyrin systems containing the zinc(II) porphyrin-free base pair (the Supporting Information[47−57] reports the complete list[58]).[7] The three main features are as follows: (1) the fastest rates are observed for rigidly held donor−acceptor systems, (2) as the spacer length increases, K_{ET} decreases, consistent with the Förster theory, and (3) the presence of aromatics at the meso-position of the porphyrin macrocycle strongly promotes energy transfer. Lindsey and collaborators have previously discussed this effect where the meso-substituted porphyrins have energy transfer rate constants greater than those of the β-substituted ones.[35] The HOMO for the meso porphyrins exhibits an a_{2u} symmetry MO in which strong electronic density is present at the meso carbon, whereas the HOMO for β-substituted ones shows an a_{1u} symmetry MO where a node is located exactly at these carbons.[36,59−61] In comparison to the collected data of Table 4, the value calculated for the cofacial bisporphyrin, (Zn)H_2DPB (K_{ET} = 21 ns^{-1}), is the fastest one in the β-substituted porphyrin series where the spacer is connected at

(47) Hsiao, J.-S.; Krueger, B. P.; Wagner, R. W.; Johnson, T. E.; Delaney, J. K.; Mauzerall, D. C.; Fleming, G. R.; Lindsey, J. S.; Bocian, D. F.; Donohoe, R. J. *J. Am. Chem. Soc.* **1996**, *118*, 11181−11193.
(48) Osuka, A.; Tanabe, N.; Kawabata, S.; Yamazaki, I.; Nishimura, Y. *J. Org. Chem.* **1995**, *60*, 7177−7185.
(49) Jensen, K. K.; van Berlekom, S. B.; Kajanus, J.; Maartensson, J.; Albinsson, B. *J. Phys. Chem. A* **1997**, *101*, 2218−2220.
(50) Yang, S. I.; Lammi, R. K.; Seth, J.; Riggs, J. A.; Arai, T.; Kim, D.; Bocian, D. F.; Holten, D.; Lindsey, J. S. *J. Phys. Chem. B* **1998**, *102*, 9426−9436.
(51) Osuka, A.; Nagata, T.; Kobayashi, F.; Zhang, R. P.; Maruyama, K.; Mataga, N.; Asahi, T.; Ohno, T.; Nozaki, K. *Chem. Phys. Lett.* **1992**, *199*, 302−308.
(52) Gust, D.; Moore, T. A.; Moore, A. L.; Leggett, L.; Lin, S.; DeGraziano, J. M.; Hermant, R. M.; Nicodem, D.; Craig, P.; Seely, G. R.; Nieman, R. A. *J. Phys. Chem.* **1993**, *97*, 7926−7931.
(53) Gust, D.; Moore, T. A.; Moore, A. L.; Kang, H. K.; DeGraziano, J. M.; Liddell, P. A.; Seely, G. R. *J. Phys. Chem.* **1993**, *97*, 13637−13642.
(54) Kawabata, S.; Yamazaki, I.; Nishimura, Y.; Osuka, A. *J. Chem. Soc., Perkin Trans. 2* **1997**, 479−484.
(55) Strachan, J.-P.; Gentemann, S.; Seth, J.; Kalsbeck, W. A.; Lindsey, J. S.; Holten, D.; Bocian, D. F. *Inorg. Chem.* **1998**, *37*, 1191−1201.
(56) Asano-Someda, M.; Kaizu, Y. *Inorg. Chem.* **1999**, *38*, 2303−2311.
(57) Hungerford, G.; Van der Auweraer, M.; J.-C., C.; Heitz, V.; Sauvage, J. P.; Pierre, J.-L.; Zurita, D. *Chem.-Eur. J.* **1999**, *5*, 2089.
(58) In this list, (Zn)H_2DPA and related compounds from Osuka's work have been omitted. We have not been able to reproduce the data.
(59) Spellane, P. J.; Gouterman, M.; Antipas, A.; Kim, S.; Liu, Y. C. *Inorg. Chem.* **1980**, *19*, 386−391.
(60) Shelnutt, J. A.; Ortiz, V. *J. Phys. Chem.* **1985**, *89*, 4733−4739.
(61) Fletcher, J. T.; Therien, M. J. *J. Am. Chem. Soc.* **2002**, *124*, 4298−4311.
(62) Seth, J.; Palaniappan, V.; Wagner, R. W.; Johnson, T. E.; Lindsey, J. S.; Bocian, D. F. *J. Am. Chem. Soc.* **1996**, *118*, 11194−11207.

Table 4. Comparison of Selected Literature Singlet−Singlet K_{ET} for ^{1}Zn(P)* → H_2(P) Processes at 298 K

Rates (ns^{-1})	Molecule	Ref.
286[a]	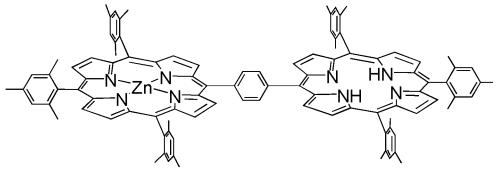	50
100	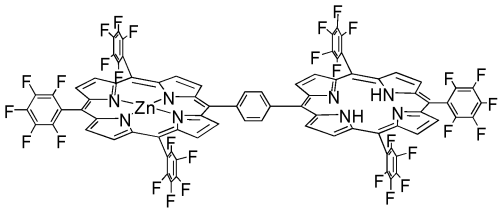	50
21	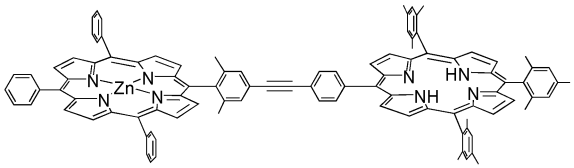	47, 62
5.8	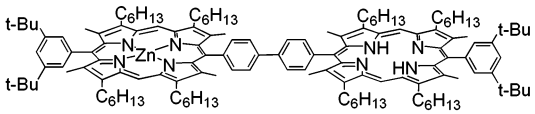	48
3.1	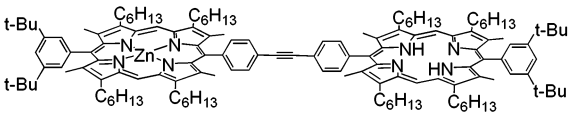	48
2.3	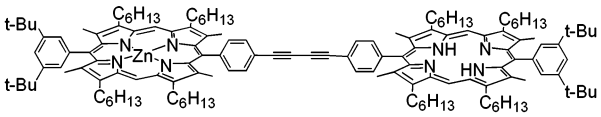	48
0.54	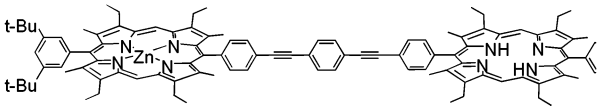	49

[a] To our knowledge, this is the fastest rate in bisporphyrin systems.

the meso-position. The short distance between the macrocycles (C_{meso}−C_{meso}) is certainly responsible for these relatively fast rates.

Conclusion

Literature works brings clear evidence that very efficient energy transfer can occur at long distances for meso-substituted porphyrins because the meso carbons exhibit a large electronic density. The energy transfer proceeds via a through-bond mechanism in such cases.[8] In β-substituted porphyrins, the weak electronic density at the meso carbons prevents any efficient energy transfer through the chemical bonds, explaining the slower rates.[36,59−61] In cofacial β-substituted bisporphyrins, the through-space transfer occurs efficiently via Dexter or Förster mechanisms. However, for β-substituted species, intermacrocycle π-orbital overlaps are required for efficient energy transfer via Dexter's mechanism. From all of these findings, cofacial meso-substituted bisporphyrins should offer an enhanced through-bond process, as well as the mechanism operating through short π-orbital overlaps. In such a case, it is anticipated that the overall rates for singlet−singlet energy transfer will be larger than that presented in this series.

Acknowledgment. P.D.H. thanks the NSERC (Natural Sciences and Engineering Research Council of Canada) for support. The support of the CNRS (R.G., UMR 5633) is also gratefully acknowledged. Marcel Soustelle (LIMSAG) is acknowledged for synthetic contributions. Prof. J. C. Scaiano and A. Aspee (University of Ottawa) are thanked for their kind help with picosecond laser fluorescence measurements.

Supporting Information Available: Table containing literature data for singlet−singlet energy transfer rate for zinc(II) porphyrin-free base diads. UV−vis spectra for H_4DPS, (Zn)H_2-DPS, and $(Zn)_2$DPS in 2-MeTHF at 77 K. Graph of K_{ET} versus $1/R^6$ and $\exp(-2R/4.8)$ for all five donor−acceptor systems in 2-MeTHF at 298 K (PDF). This material is available free of charge via the Internet at http://pubs.acs.org.

JA0379823